IEEE Photonics Journal
An IEEE Photonics Society Publication

Open Access

Arc-Induced Long Period Gratings in Erbium-Doped Fiber

Volume 11, Number 1, February 2019

Flavio Esposito
Stefania Campopiano
Agostino Iadicicco

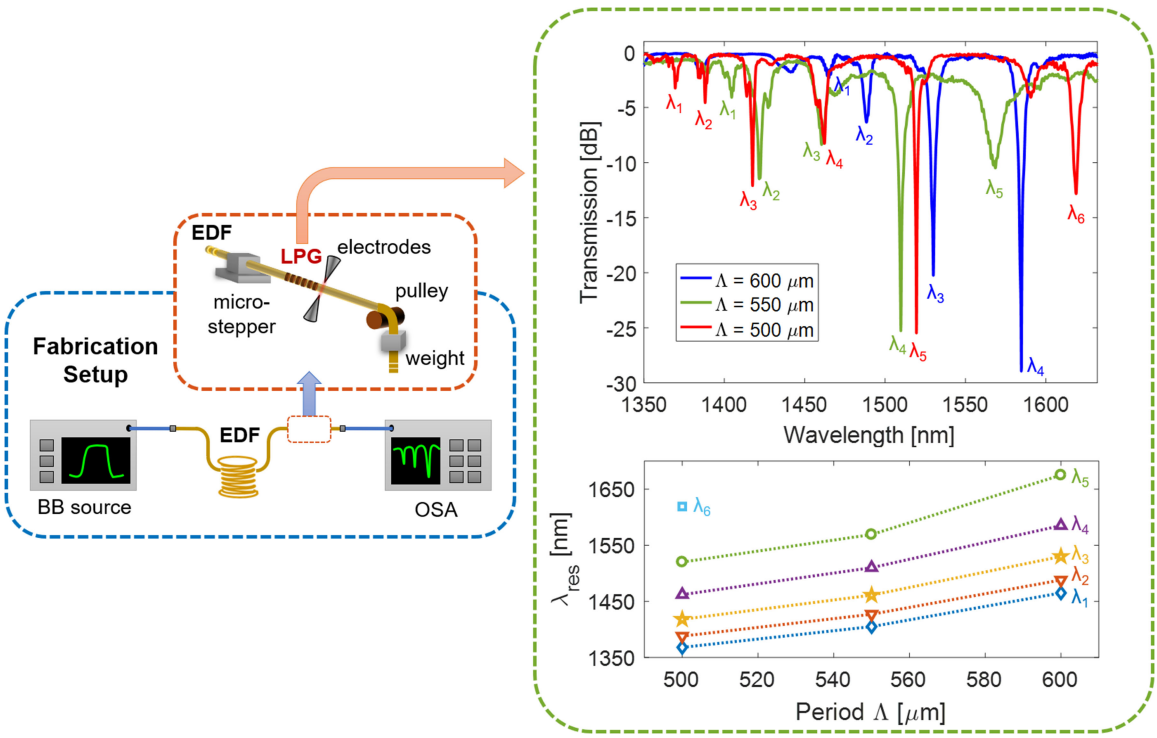

DOI: 10.1109/JPHOT.2019.2894300
1943-0655 © 2019 IEEE

Arc-Induced Long Period Gratings in Erbium-Doped Fiber

Flavio Esposito, Stefania Campopiano, and Agostino Iadicicco

Department of Engineering, University of Naples "Parthenope ", Naples 80143, Italy

DOI:10.1109/JPHOT.2019.2894300

Manuscript received December 4, 2018; accepted January 16, 2019. Date of publication January 21, 2019; date of current version February 8, 2019. This work was supported by the University of Naples "Parthenope" through the "Bando di sostegno alla ricerca individuale per triennio 2015-2017, Annualità 2017." Corresponding author: Agostino Iadicicco (e-mail: iadicicco@uniparthenope.it).

Abstract: In this paper, we report about the fabrication of long period gratings (LPGs) directly into an Erbium-doped fiber, by using the electric arc discharge technique. The attention is focused on the writing process and the resulting properties, by considering gratings with different periods and measuring their spectra over a wide wavelength range. The LPGs show high order attenuation bands with tunable resonance wavelengths and depths up to 30 dB, while the lengths of the final devices are in range 20–45 mm. The polarization-dependent loss of these LPGs is also measured, for the first time in this kind of fiber. As further novelty, the influence of surrounding refractive index, applied strain, and temperature is investigated and discussed in comparative manner. Based on the achieved results, this fabrication procedure can be adapted to a specific application, for example in optical communications, signal processing, and sensing fields.

Index Terms: Fiber gratings, fiber optics systems, sensors, waveguide devices.

1. Introduction

The Long Period Grating (LPG) is a fiber optic device, consisting of a periodic modulation of the refractive index and/or the geometry of the fiber, with period typically between 100 μm and 1 mm. Such perturbation results in the power coupling between the core mode and co-propagating cladding modes, at specific resonance wavelengths given by the following phase-matching condition [1]:

$$\lambda_i = \left(n_{eff,co} - n_{cl,i}\right) \cdot \Lambda \tag{1}$$

where $n_{eff,co}$ is the effective refractive index of the core mode, $n_{cl,i}$ is the effective refractive index of the ith cladding mode and Λ is the grating period. The resulting transmission spectrum of the fiber thus exhibits a series of attenuation bands, that are located at those resonance wavelengths. Due to such spectral shape, the LPG finds wide application in optical communications, signal processing and sensing fields [2]–[5]. First examples were fabricated in the standard single mode fiber (SMF), by exploiting the photosensitivity of the Germanium-doping when exposed to an UV radiation through a periodic amplitude mask [2].

Fiber dopants, indeed, play a dominant role when designing optical fibers with novel and specific physical and optical properties, such as the refractive index contrast, absorption/emission bands, melting properties, radiation resistance and more. On this line of argument, several unconventional fibers have been developed in the past years for specific applications. However, they often present

low or null photosensitivity, thus there is a need of grating writing procedures that do not rely on such property, as for example the Electric Arc Discharge (EAD) technique [6], [7].

EAD demonstrated high flexibility and reduced cost when applied to the fabrication of LPGs. Here, the grating is thermo-induced in the fiber, by applying an electric arc with a periodic step: when the fiber is subjected to such high temperature, its geometrical and physical properties are modified [6]. As a result, the fabrication of arc-induced LPGs was successfully demonstrated in optical fibers with different dopants including, but not limited to, Fluorine, Nitrogen, Aluminum, Sulphur, and Phosphorous [7]–[12]. At the same time, the optimization of the EAD procedure makes it a real concurrent approach, for the LPG fabrication beyond the photosensitivity limitation, as testified for example by the recent results in polarization-maintaining Panda fiber [13], [14].

Among specialty ones, Erbium-doped fibers (EDFs) belong to the category of rare-earth-doped or active optical fibers, which are typically used for the realization of amplifiers in the 1.5 μm wavelength region [15]. Different studies focused on the advantages connected to the direct inscription of LPGs in such active medium, finding improved gain characteristics. For example: in [16], [17] novel gain flattening techniques of Er-doped fiber amplifiers (EDFAs), with enhanced gain, were presented; a theoretical scheme for a novel high-power LPG-assisted EDFA was reported in [18]; an all-optical lossless differentiator was presented as well [19]. Finally, fibers containing Erbium have been studied also for which concerns their behavior under the effect of radiations [20], [21].

However, despite their potentialities, there are only few experimental reports of LPGs directly written into Er-doped fibers. In [22], [23] it was shown that, for a CO_2 written LPG, the transmission characteristics can be tuned through the pump power of laser source. The effect of pump gain over a grating resonance was investigated also for an UV-LPG in [24], but in this case the fiber was pre-hydrogenated to present photosensitivity. It should be stressed that, in these works, the attention does not focus on the writing process but mostly on the effect of pump power. In fact, the spectra of the LPGs presented in [22], [23] are reported in a wavelength range that in the best case is not higher than 60 nm, resulting in a single attenuation band visible. Finally, in [9] the temperature response of LPGs induced in Al/Er-codoped through EAD and mechanical micro-bends (i.e., reversible grating) were considered. Hence, to our knowledge, there is no comparative investigation between such LPGs at different period and their polarization-dependent loss (PDL) remains still unexplored. Finally, their behavior under different strain and surrounding refractive index (SRI) conditions has not been reported as well.

In this scenario, in this work we report about the fabrication of Long Period Gratings into an Er-doped fiber, by means of the Electric Arc Discharge technique, focusing the attention on the writing conditions and subsequent grating properties. The achieved experimental results demonstrate that the EAD technique allows the fabrication of LPG in Er-doped fiber with a full control of the spectral features, in terms of depth of the attenuation bands, spectral position of the attenuation bands and tuning on the bandwidth. This feature is widely desired in specialty applications of gratings in Er-doped fibers [16], such as flattening of optical sources. As well as the control of spectral characteristics is welcome in sensing applications. Moreover, such result is not dependent on the photosensitivity characteristics of the fiber. In particular, LPGs with different periods Λ are considered and their spectra being reported over a wide wavelength range. In addition, the PDL of the gratings was also investigated, for the first time in this kind of fiber. Finally, as further novelty, the influence of SRI, applied strain and temperature are also comparatively investigated and discussed.

2. Methods and Results

2.1 Fabrication of the LPGs in Er-Doped Fiber

The schematic of the fabrication platform, based on the electric arc discharge technique, herein discussed is reported in Fig. 1, and additional details can be found in [7] as well. It is a step-by-step procedure aimed to create a sequence of perturbations within the fiber, each one acting on both its physical and geometrical features. The single perturbation is achieved by means of a fast and localized temperature increase, due to the discharge occurring between the two electrodes. As

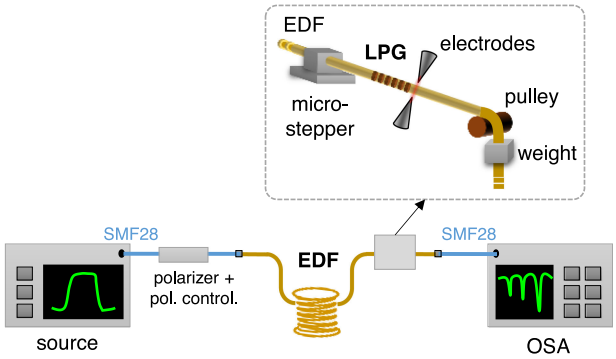

Fig. 1. Schematic of the setup for the fabrication of LPGs based on Electric Arc Discharge technique.

a result, a tapering of the transversal size of the fiber and a change in the silica refractive index as consequence of stress relaxation is created [6]. In order to replicate the single perturbation in controllable manner, the EAD is combined with a mechanical action, i.e., it is typically applied with the fiber subjected to a constant axial tension.

In our case, we used the electrodes of a commercial fusion splicer (model Type-39 by Sumitomo Electric, Japan), which was modified to have the control of the discharge parameters and fiber alignment. The selection of the arc power, arc duration, electrodes distance, and fiber tension allows the regulation of the modulation strength and thus of the LPG spectral features. Typical values for the arc power are in range 1–25 step (proprietary unit from manufacturer), arc times of 200–900 ms, 0.8–2.0 mm for the electrodes gap, while for the pulling tension a weight of 10–15 g is used. As depicted in Fig. 1, the setup presents a micro-stepper, which is used for the fiber displacement of the grating period Λ. During the fabrication, on-line spectral monitoring of the fiber is also performed, by illuminating it with a broadband source (with wavelength range of 1100–1700 nm) and measuring the output through an optical spectrum analyzer OSA (AQ6370B, Yokogawa, Japan, with resolution of 0.1 nm in our case). Moreover, a polarizer (type ILP1550SM, Thorlabs, USA) and polarization controller (FPC562, Thorlabs) are connected after the source, in order to change the light state of polarization at the input of the fiber, when required.

For the purpose of the work, we have selected the M5–980–125 Er-doped fiber by Fibercore, which is proposed for the manufacturing of EDFAs. The fiber has $D_{clad} = 125.0\ \mu$m, MFD $= 5.5$–$6.3\ \mu$m at $\lambda = 1550$ nm, NA $= 0.21$–0.24, $\lambda_{cut} = 900$–970 nm and an estimated $D_{core} \sim 3.2\ \mu$m. The absorption at $\lambda = 1531$ nm is $\sim$7 dB/m, which classifies this fiber among the ones with relatively low Erbium content. Due to the high attenuation, a 100-150 cm long section of the fiber was spliced between two SMF28 pigtails by manual procedure, to minimize splicing losses.

Here, LPGs have been successfully fabricated using the following parameters: arc power $= 20$ step, arc time $= 700$ ms, electrodes gap $= 0.8$ mm and weight $= 12.0$ g. As a result, Fig. 2(a) reports the transmission spectra (under unpolarized light) of a LPG with period $\Lambda = 600\ \mu$m fabricated in a 130 cm long section of this EDF, as function of grating length (in terms of number or periods). As one can observe, the step-by-step nature of the EAD technique permits an easy control of the depth of the attenuation bands by acting on the number of periods [12]. For the aim of this paper, we stopped the fabrication after 39 arcs, i.e., for a total length of the device L $= 23.4$ mm. Four attenuation bands, λ_1, λ_2, λ_3, and λ_4, are clearly visible in the wavelength range under investigation, which can be associated to the coupling with LP_{02}, LP_{03}, LP_{04}, and LP_{05} cladding mode, respectively. In particular, λ_3 is located at 1530.0 nm (i.e., around the Erbium emission wavelength) with depth of 20.2 dB, while λ_4 is positioned at 1584.7 nm with high depth of 29.0 dB. It is interesting to highlight that, if compared to SMF28 fiber [7], for a given period, here the maximum cladding mode order is higher, due to the combination of lower core diameter and higher refractive index contrast between core and cladding regions (i.e., higher NA).

In similar manner, Fig. 2(b) and 2(c) report the spectra of two other LPGs manufactured in the same fiber with $\Lambda = 550\ \mu$m and $\Lambda = 500\ \mu$m, respectively, during the fabrication process. In this

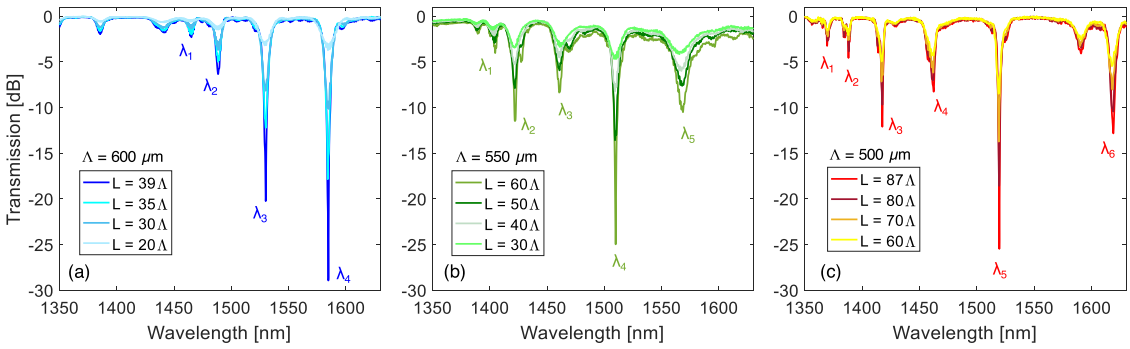

Fig. 2. Transmission spectrum during fabrication process of LPG with period Λ of: (a) 600 μm; (b) 550 μm; (c) 500 μm.

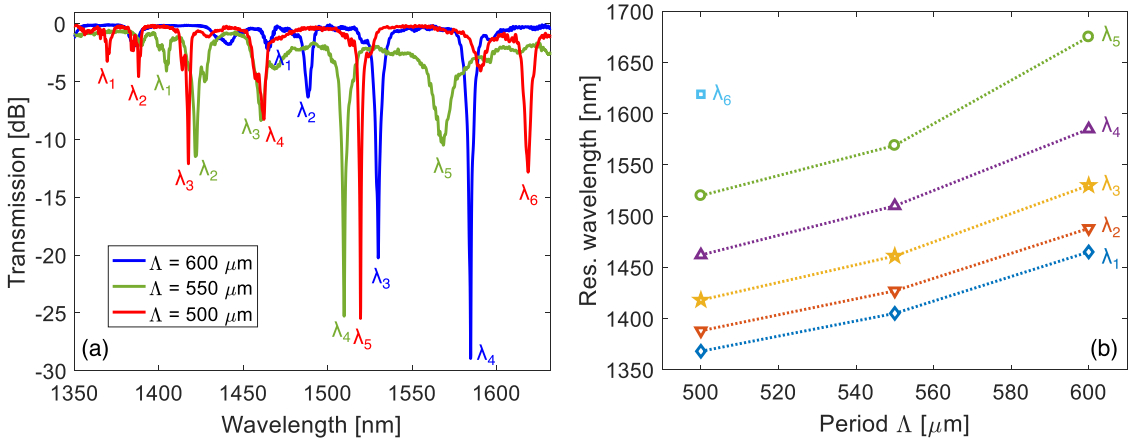

Fig. 3. Comparison of LPGs in Er-doped fiber: (a) spectrum for different grating period; (b) resonance wavelengths versus period.

case, the final length of the devices were 33.0 mm and 43.5 mm, respectively, and in the same wavelength range the number of attenuation bands increases as the period is decreased. In fact, concerning the LPG with 550 μm period, we can see λ_4 located at 1509.8 nm with depth of 25.3 dB and λ_5 at 1568.6 nm with depth of 10.5 dB. While, for the LPG with $\Lambda = 500$ μm, the λ_5 is located at 1519.5 nm with depth of 25.5 dB and λ_6 at 1618.8 nm with 13.0 dB depth. These depths are among the highest for a LPG fabricated in this kind of fiber by means of any fabrication procedure, without any pump source [9], [23], [24], moreover the possibility of selecting such depth in a wide range trough the number of arcs is clearly demonstrated.

The spectra of the three LPGs are comparatively reported in Fig. 3(a) and it is worth highlighting that is the first time that spectra of LPGs in Er-doped fiber at different periods are presented and compared over a wide wavelength range. For further analysis, we have reported in Fig. 3(b) the corresponding phase-matching curves, relating the spectral position of the resonance wavelengths to the period. As one can observe, according to the theoretical behavior [2], the resonance wavelengths increases with Λ. The slope of such trends increases with mode order, demonstrating the consistency and reproducibility of the results. For example, it changes from $\partial\lambda_1/\partial\Lambda = 1.97$ nm/μm to $\partial\lambda_5/\partial\Lambda = 1.55$ nm/μm in the range $\Lambda = 500$–600 μm, considering a linear approximation. The aim of the results reported in Fig. 3(b) is to permit the tuning of the spectral position of the attenuation band of interest to a specific wavelength.

Concerning the physical mechanisms involved in grating formation, it is important to remark that it was seen that the EAD procedure can act on dopant diffusion, stress relaxation, waveguide

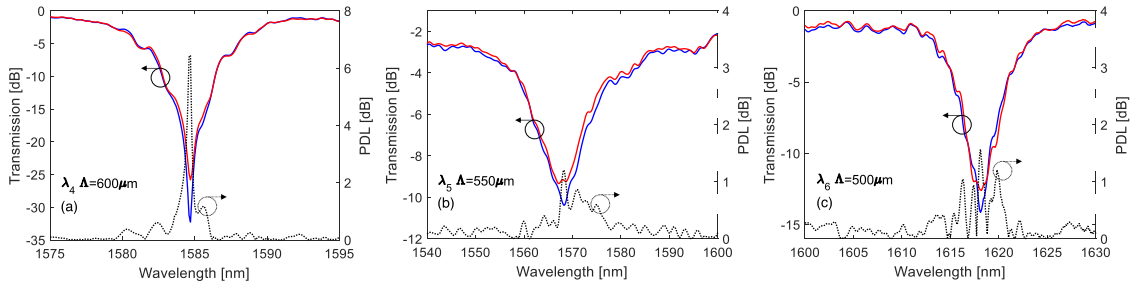

Fig. 4. Transmission spectrum of LPG for minimum (blue) and maximum (red) transmission, and PDL (black) for: (a) λ_4 and $\Lambda = 600$ μm; (b) λ_5 and $\Lambda = 550$ μm; (c) λ_6 and $\Lambda = 500$ μm.

geometry, and on glass structure. In most case, the identification of the predominant one is still an open point, and it was seen that is highly dependent on the writing conditions and on the fiber type [6]. Similarly to the grating in standard fiber, we believe that the main effect of the grating formation in this fiber is the refractive index change due to the stress relaxation, as also pointed out for Al/Er-doped fibers in [9].

Based on these results, we have been able to demonstrate that, despite the additional challenges related to EDF properties, the procedure enables the fabrication of LPGs with fine control of their spectral features (in terms of spectral position, depth and bandwidth), with the possibility to be adapted for a specific application.

2.2 Polarization-Dependent Loss Measurement

This section reports on the polarization properties of the gratings, as in general their performance in both telecommunications and sensing systems are affected by the intrinsic polarization-dependent loss [25]. In particular, the PDL originates from the birefringence that is present in the grating structure, and therefore, the grating transmission properties can depend upon the light polarization state [26]. It should be remarked here that such measurements were never performed on LPGs in EDF. By means of the setup reported in Fig. 1, the input light was linearly polarized through the polarizer; subsequently the polarization state was afterwards scanned by the polarization controller, before going through the LPG and be acquired by the OSA. Hence, the maximum and minimum transmitted power, within the wavelength range around the resonance wavelength of a specific cladding mode, are measured. Finally, the PDL was obtained by computing the absolute difference of maximum and minimum transmission [27].

In Fig. 4(a) we have reported the maximum (red line) and minimum (blue line) transmission spectra of the LPG with $\Lambda = 600$ μm, focusing on the cladding mode λ_4. Considering that the PDL_{max} of a LPG is defined as the maximum PDL around the resonance wavelength of the attenuation band, it can be observed from the dotted line that in this case $PDL_{max} = 6.4$ dB for a band with an attenuation around 30 dB. Whereas concerning the difference in resonance wavelength position between the two cases, it is below 0.1 nm.

In Fig. 4(b) and 4(c) we have reported, respectively, the PDL around the mode λ_5 in the LPG with $\Lambda = 550$ μm and λ_6 for $\Lambda = 500$ μm. In this case, for λ_5 (having depth $\sim$10 dB) the lowest $PDL_{max} = 1.2$ dB was obtained, while for λ_6 ($\sim$13 dB depth) it is slightly higher and equal to $PDL_{max} = 1.6$ dB. The difference in resonance wavelength position, between the maximum and minimum transmission case, is comprised here in 0.1-0.4 nm. It should be recalled that the lower values of PDL_{max} are in agreement with the lower transmission loss of the corresponding attenuation bands [25].

As overall assessment, these values are comparable with respect to those of LPGs fabricated in standard fibers by EAD technique (without any reduction technique), for which the PDL_{max} was in between 1–12 dB [25], [28]. Anyway, it should be also pointed out that, as the PDL is highly

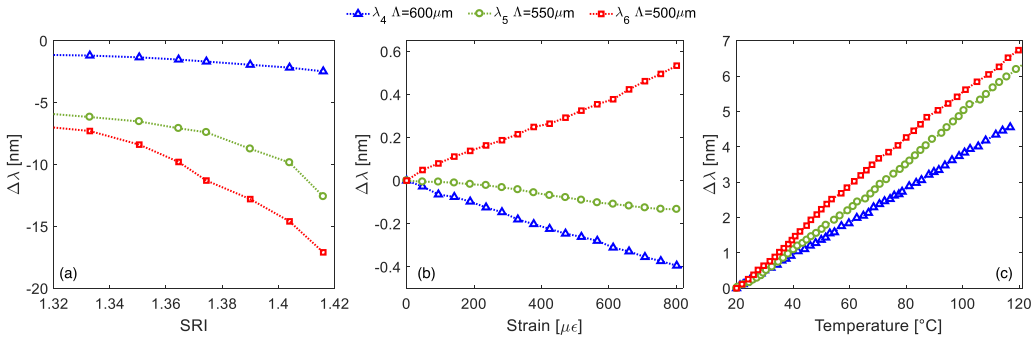

Fig. 5. Resonance wavelength shift of different cladding modes in EDF-LPGs, induced by changes in: (a) SRI, (b) applied strain and (c) temperature.

dependent on the LPG spectral features (and thus the fabrication parameters of arc power, arc time and pulling tension), in principle such parameters could be further adjusted to reduce the PDL.

2.3 Investigation on the Influence of External Parameters

Here, we present and discuss the influence of surrounding refractive index, applied strain, and temperature over these LPGs, by focusing the attention on the highest order mode.

For the characterization with respect to SRI, the LPG was tested by placing it into liquids with different refractive index, based on aqueous solutions of glycerin at different concentration, in the range $n_{SRI} = 1.33$–1.42 (measured at $\lambda = 589$ nm and T = 20 °C by Abbe refractometer with resolution of 10^{-3} RIU). During the procedure, the grating was kept under constant tension (120 mN) and temperature (20 °C) conditions, using the setup reported in [7]. The resonance wavelength shifts obtained for the different LPGs are thus reported in Fig. 5(a) (each curve is normalized with respect to the value at $n_{SRI} = 1.0$), after post-processing of spectrum data based on centroid analysis. As one can observe, the increase in external refractive index produces a blue shift of the resonance wavelengths, with sensitivity increasing with SRI and mode order [1]. Such response arises from the dependence of the effective refractive index of the cladding modes with SRI. In particular, concerning the resonance λ_4 of the LPG with $\Lambda = 600$ μm, a shift $\Delta\lambda_4$ of -1.2 nm was recorded for $n_{SRI} = 1.333$ (water), which increases to -2.5 nm for $n_{SRI} = 1.416$. While, for the λ_5 (for $\Lambda = 550$ μm) higher values $\Delta\lambda_5$ of -6.2 nm and -12.6 nm were recorded for the same SRIs. Finally, the band λ_6 ($\Lambda = 500$ μm) exhibited even higher values $\Delta\lambda_6$ of -7.3 nm and -17.1 nm, respectively. We found that such values are slightly lower, if compared to same order cladding modes for LPGs in SMF28. In fact, in standard fiber, considering a 6th order cladding mode we measured shifts of -10.7 nm and -21.9 nm, for SRI of 1.333 and 1.416, respectively [29].

Concerning the measurement of strain induced effects, the setup is arranged as in [7], where one fiber end is fixed on the top of an holder, while to the other one is subjected to axial force, resulting in strain variations up to 800 $\mu\varepsilon$ (temperature and SRI were kept constant). The tension is created by the application of weights through a pulley, and a Fiber Bragg Grating (FBG) is used as reference. The resonance wavelength shifts as function of applied strain are reported in Fig. 5(b), where one can observe that the behavior can be approximated by linear dependence (mean $R^2 = 0.9913$) in the range under investigation. In particular, the following sensitivities were measured: $S_{\varepsilon,4} = \partial\lambda_4/\partial\varepsilon = -0.5$ pm/$\mu\varepsilon$, $S_{\varepsilon,5} = -0.2$ pm/$\mu\varepsilon$, and $S_{\varepsilon,6} = 0.6$ pm/$\mu\varepsilon$. In this case, the wavelength shift is the sum of a material contribution (i.e., strain dependence of the effective refractive indices) and a waveguide effect (variation of the grating period with strain). Both affect significantly the strain response and the balance between the two terms is strongly dependent on the cladding mode order. As a result, the overall response is typically negative for lower order modes and positive for higher order ones [1]. In SMF28 we have measured higher strain sensitivity for λ_6 around 1.5 pm/$\mu\varepsilon$, as such sensitivity is strongly influenced by the fiber composition.

To conclude, the temperature dependence was investigated as well in the range 20–120 °C. For the purpose, the LPG was placed in a tubular oven with a FBG as reference, as reported in [7], while kept under constant 120 mN pulling tension. The temperature dependence is mostly related to the material contribution, since in this case the waveguide effect presents trivial influence [1]. As one can observe from Fig. 5(c), the responses exhibited linear behavior in the range considered, resulting in the following sensitivities $S_{T,4} = \partial\lambda_4/\partial T = 47.1$ pm/°C, $S_{T,5} = 63.7$ pm/°C, and $S_{T,6} = 68.8$ pm/°C with mean $R^2 = 0.9984$. Such values are comparable with the sensitivity of 60 pm/°C reported for the LPG in Al/Er-codoped fiber reported in [9], while being lower for example than the 80 pm/°C sensitivity we found for 6th order cladding mode in SMF28.

3. Conclusions

In this paper, we have reported about the fabrication of LPGs directly into the M5–980–125 Er-doped fiber manufactured by Fibercore, by using the electric arc discharge technique. These gratings were obtained with tunable attenuation bands having attenuation up to 30 dB, length in range 20–45 mm, and coupling to higher order modes. The samples presented here were fabricated by using different grating periods Λ, and their polarization properties in terms of PDL were studied for the first time in an EDF. Subsequently, as additional novelty, their behavior under changes in the surrounding refractive index, strain, and temperature conditions was investigated and discussed. Based on the achieved possibility of fine tuning the LPG spectral features, this fabrication procedure can be adapted for a specific application, as for example in communications, signal processing and optical metrology fields. As a concrete perspective, we are going to test similar LPG samples written in EDF under ionizing radiations based on two main considerations: i) we have recently demonstrated the feasibility of a gamma dosimeter based on LPG written in unconventional fibers [30]; ii) there is interest in the radiation sensitivity of EDFs, as testified by different works [20], [21], [31].

References

[1] V. Bhatia, "Applications of long-period gratings to single and multi-parameter sensing," *Opt. Exp.*, vol. 4, no. 11, pp. 457–466, 1999.

[2] S. W. James and R. P. Tatam, "Optical fibre long-period grating sensors: Characteristics and application," *Meas. Sci. Technol.*, vol. 14, no. 5, pp. R49–R61, 2003.

[3] S. Ramachandran *et al.*, "All-fiber grating-based higher order mode dispersion compensator for broad-band compensation and 1000-km transmission at 40 Gb/s," *IEEE Photon. Technol. Lett.*, vol. 13, no. 6, pp. 632–634, Jun. 2001.

[4] F. Esposito *et al.*, "Single-ended long period fiber grating coated with polystyrene thin film for butane gas sensing," *J. Light. Technol.*, vol. 36, no. 3, pp. 825–832, Feb. 2018.

[5] F. Esposito, L. Sansone, C. Taddei, S. Campopiano, M. Giordano, and A. Iadicicco, "Ultrasensitive biosensor based on long period grating coated with polycarbonate-graphene oxide multilayer," *Sensors Actuators B Chem.*, vol. 274, pp. 517–526, Nov. 2018.

[6] G. Rego, "Arc-induced long period fiber gratings," *J. Sensors*, vol. 2016, 2016, Art. no. 3598634.

[7] F. Esposito, R. Ranjan, S. Campopiano, and A. Iadicicco, "Arc-induced long period gratings from standard to polarization-maintaining and photonic crystal fibers," *Sensors*, vol. 18, no. 3, 2018, Art. no. 918.

[8] G. Rego, O. Okhotnikov, E. Dianov, and V. Sulimov, "High-temperature stability of long-period fiber gratings produced using an electric Arc," *J. Light. Technol.*, vol. 19, no. 10, pp. 1574–1579, Oct. 2001.

[9] G. Rego *et al.*, "Arc-induced long-period gratings in aluminosilicate glass fibers," *Opt. Lett.*, vol. 30, no. 16, pp. 2065–2067, Aug. 2005.

[10] F. Durr *et al.*, "Tomographic stress profiling of arc-induced long-period fiber gratings," *J. Light. Technol.*, vol. 23, no. 11, pp. 3947–3953, Nov. 2005.

[11] G. Humbert, A. Malki, S. Février, P. Roy, and D. Pagnoux, "Characterizations at high temperatures of long-period gratings written in germanium-free air–silica microstructure fiber," *Opt. Lett.*, vol. 29, no. 1, pp. 38–40, Jan. 2004.

[12] R. Ranjan, F. Esposito, A. Iadicicco, and S. Campopiano, "Arc-induced long period gratings in phosphorus-doped fiber," *IEEE Photon. Technol. Lett.*, vol. 29, no. 7, pp. 611–614, Apr. 2017.

[13] A. Iadicicco, R. Ranjan, F. Esposito, and S. Campopiano, "Arc-induced long period gratings in polarization-maintaining panda fiber," *IEEE Photon. Technol. Lett.*, vol. 29, no. 18, pp. 1533–1536, Sep. 2017.

[14] R. Ranjan, F. Esposito, S. Campopiano, and A. Iadicicco, "Sensing characteristics of arc-induced long period gratings in polarization-maintaining panda fiber," *IEEE Sens. J.*, vol. 17, no. 21, pp. 6953–6959, Nov. 2017.

[15] C. R. Giles and E. Desurvire, "Modeling erbium-doped fiber amplifiers," *J. Light. Technol.*, vol. 9, no. 2, pp. 271–283, Feb. 1991.

[16] R. Singh, S. Vashisth, and E. K. Sharma, "Gain flattening by long period gratings in erbium doped fibers," *Opt. Commun.*, vol. 240, pp. 123–132, Oct. 2004.

[17] I. B. Sohn and J. W. Song, "Gain flattened and improved double-pass two-stage EDFA using microbending long-period fiber gratings," *Opt. Commun.*, vol. 236, no. 1–3, pp. 141–144, 2004.
[18] G. Nemova and R. Kashyap, "High-power long-period-grating-assisted erbium-doped fiber amplifier," *J. Opt. Soc. Amer. B*, vol. 25, no. 8, pp. 1322–1327, Aug. 2008.
[19] D. Krcmarík, R. Slavík, Y. Park, M. Kulishov, and J. Azaña, "First-order loss-less differentiators using long period gratings made in Er-doped fibers," *Opt. Exp.*, vol. 17, no. 2, pp. 461–471, Jan. 2009.
[20] P. Borgermans *et al.*, "Dosimetry with optical fibers: Results for pure silica, phosphorous, and erbium doped samples," *Proc. SPIE*, vol. 4204, pp. 151–160, 2001.
[21] M. C. Paul, R. Sen, S. K. Bhadra, and K. Dasgupta, "Radiation response behaviour of Al codoped germano-silicate SM fiber at high radiation dose," *Opt. Commun.*, vol. 282, no. 5, pp. 872–878, 2009.
[22] R. Slavík and M. Kulishov, "Active control of long-period fiber-grating-based filters made in erbium-doped optical fibers," *Opt. Lett.*, vol. 32, no. 7, pp. 757–759, Apr. 2007.
[23] D. Krcmarik, R. Slavik, M. Karasek, and M. Kulishov, "Theoretical and experimental analysis of long-period fiber gratings made directly into Er-doped active fibers," *J. Light. Technol.*, vol. 27, no. 13, pp. 2335–2342, Jul. 2009.
[24] A. Quintela, M. A. Quintela, C. Jauregui, and J. M. Lopez-Higuera, "Optically tunable long-period fiber grating on an Er3+ Fiber," *IEEE Photon. Technol. Lett.*, vol. 19, no. 10, pp. 732–734, May 2007.
[25] G. M. Rego, J. L. Santos, and H. M. Salgado, "Polarization dependent loss of arc-induced long-period fibre gratings," *Opt. Commun.*, vol. 262, no. 2, pp. 152–156, Jun. 2006.
[26] B. L. Bachim and T. K. Gaylord, "Polarization-dependent loss and birefringence in long-period fiber gratings," *Appl. Opt.*, vol. 42, no. 34, pp. 6816–6823, Dec. 2003.
[27] Yihong Zhu, E. Simova, P. Berini, and C. P. Grover, "A comparison of wavelength dependent polarization dependent loss measurements in fiber gratings," *IEEE Trans. Instrum. Meas.*, vol. 49, no. 6, pp. 1231–1239, Dec. 2000.
[28] F. D. S. Delgado, A. B. dos Santos, and A. Bessa, "Reduction of intrinsic polarization dependence in arc-induced long-period fiber gratings," *Opt. Eng.*, vol. 57, no. 6, Jun. 2018, Art. no. 067105.
[29] F. Esposito, R. Ranjan, S. Campopiano, and A. Iadicicco, "Experimental study of the refractive index sensitivity in arc-induced long period gratings," *IEEE Photon. J.*, vol. 9, no. 1, Feb. 2017, Art. no. 7100110.
[30] A. Stăncălie *et al.*, "Long Period Gratings in unconventional fibers for possible use as radiation dosimeter in high-dose applications," *Sensors Actuators A Phys.*, vol. 271, pp. 223–229, Mar. 2018.
[31] A. Morana *et al.*, "Femtosecond IR laser inscription and X-ray radiation response of fiber Bragg gratings in aluminosilicate optical fibers," in *Proc. Adv. Photon. 2018 (BGPP, IPR, NP, NOMA, Sensors, Networks, SPPCom, SOF)*, 2018, Paper BM2A.2.